



RARE DECAY OF \bar{B}^0 MESON TO \bar{K}^{*0} AND LEPTON PAIR

A. Yu. Korchin^a, V. A. Kovalchuk^b, D. O. Lazarenko^c

Akhiezer Institute for Theoretical Physics, NSC “Kharkov Institute of Physics and Technology”, Kharkov 61108, Ukraine

Branching ratio and other observables for the rare flavour-changing neutral current decay $\bar{B}_d^0 \rightarrow \bar{K}^{*0} (\rightarrow K^- \pi^+) e^+ e^-$ are studied below $\bar{c}c$ threshold. The total amplitude for this decay includes the term coming from the Standard Model effective Hamiltonian and the term generated by the processes $\bar{B}_d^0 \rightarrow \bar{K}^{*0} (\rightarrow K^- \pi^+) V$ with intermediate low-lying vector resonances $V = \rho(770), \omega(782), \phi(1020)$ decaying into the $e^+ e^-$ pair. Influence of the resonances in the region of electron-positron invariant mass up to 2.5 GeV is studied in view of measurements on LHCb.

1 Introduction

The investigation of rare B decays induced by the flavour-changing neutral current (FCNC) transitions $b \rightarrow s$ and $b \rightarrow d$ represents an important test of the Standard Model (SM) or its extensions (see [1] for a review). Among the rare decays, the radiative decay $b \rightarrow s\gamma$ has probably been the most popular FCNC transition ever since its experimental observation as $B \rightarrow K^*\gamma$ at CLEO in 1993 [2]. This decay proceeds through a loop (penguin) diagram, to which high-mass particles introduced in extensions to the SM may contribute with a sizeable amplitude. The size of the decay rate itself, however, provides only a mild constraint on such extensions, because the SM predictions for exclusive rates suffer from large and model dependent form factor uncertainties [3, 4]. Further reduction in the theory errors appears rather difficult. Therefore it is advantageous to use in addition to the rates other observables that can reveal New Physics (NP).

In particular, in framework of the SM, the photons emitted in $b \rightarrow s\gamma$ decays are predominantly left-handed, while those emitted in \bar{b} decay are predominantly right-handed. The amplitude for emission of wrong-helicity photons is suppressed by a factor $\propto m_s/m_b$ [5], but this suppression can easily be alleviated in a large number of NP scenarios where the helicity flip occurs on an internal line.

Measurement of the photon helicity is therefore of interest. Several different methods of measuring the photon polarization have been suggested, however it appears that the photon polarization is difficult to measure, and one has to use rather the process $b \rightarrow s\gamma^* \rightarrow s\ell^+\ell^-$, where the photon is converted to the lepton pair. In this decay the angular distributions and lepton polarizations can probe the chiral structure of the matrix element [6, 7, 8, 9, 10, 11, 12] and thereby the NP effects.

In order to measure effects of NP in the process $b \rightarrow s\ell^+\ell^-$ one needs to calculate the SM predictions with a rather good accuracy. The SM amplitude consists of the short-distance (SD) contribution and the long-distance (LD) ones. The former is expressed in terms of the Wilson coefficients C_i calculated in perturbative QCD; they carry information on processes at energy scale $\sim m_W, m_t$. These coefficients are then evolved using the renormalization group methods to the energies related to the bottom quark mass m_b .

The LD terms include factorizable and non-factorizable effects from virtual photon via the semi-leptonic operators $\mathcal{O}_{9V, 10A}$ and electromagnetic dipole penguin operator $\mathcal{O}_{7\gamma}$ in effective Hamiltonian. The radiative corrections coming from operators \mathcal{O}_{1-6} and gluon penguin operator \mathcal{O}_{8g} are also accounted for [13].

The LD effects describing the hadronization process are expressed in terms of matrix elements of the $b \rightarrow s$ operators between the initial B and the K^* final state. These matrix elements are parameterized in terms of form factors [8] that are calculated with the help of light-cone sum rules (LCSR) [14] or in soft-collinear effective theory (SCET) [15]. The form factors have large theoretical uncertainties that are presently the dominant uncertainties in the SM predictions for exclusive decays.

The presence of additional LD effects originating from intermediate vector resonances $\rho(770), \omega(782), \phi(1020), J/\psi(1S), \psi(2S), \dots$ complicates the description. These resonances show up in the region of relatively small dilepton invariant mass $m_{ee} \equiv \sqrt{q^2}$, where $q^2 = (q_+ + q_-)^2$. In order to suppress the charmonia contribution, often the region of large dilepton mass ($q^2 \gg 4m_c^2 \approx 6.5 \text{ GeV}^2$) is selected, for example, BaBar and Belle Collaborations apply the corresponding experimental cuts [16, 17].

The region of small dilepton invariant mass, $m_{ee} < 1 \text{ GeV}$, has also high potential of searching effects of the NP [6]. At small $m_{ee} \sim M_R$ the low-lying vector resonances modify the amplitude, and thus may induce in certain observables the right-handed photon polarization, which is still small but not negligible. The presence of

e-mail: ^akorchin@kipt.kharkov.ua, ^bkoval@kipt.kharkov.ua, ^cdenis.lazarenko@gmail.com

© Korchin A.Yu., Kovalchuk V.A., Lazarenko D.O. , 2011.

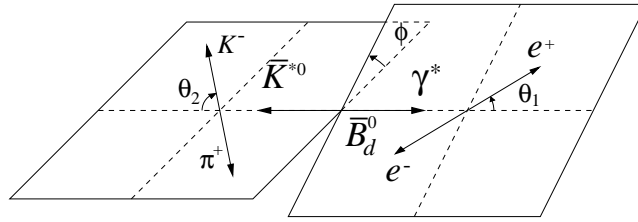


Figure 1. Definition of helicity angles θ_1 , θ_2 , and ϕ , for the decay $\bar{B}_d^0 \rightarrow \bar{K}^{*0} e^+ e^-$.

the photon propagator $1/q^2$ enhances the resonance contribution. Recently the authors of [18] analyzed angular distribution in the rare decay $\bar{B}^0 \rightarrow \bar{K}^{*0} e^+ e^-$ in the small- q^2 region in order to test possibility to measure this distribution at LHCb.

We study the $\bar{B}^0 \rightarrow \bar{K}^{*0} e^+ e^-$ decay at dilepton invariant mass $m_{ee} < 2.5$ GeV. Both the SD and LD effects in the amplitude are evaluated. The effective Hamiltonian with the Wilson coefficients in next-to-next-to-leading order (NNLO) approximation is used. The LD effects mediated by the resonances, *i.e.* $\bar{B}^0 \rightarrow \bar{K}^{*0} V \rightarrow \bar{K}^{*0} \gamma^* \rightarrow \bar{K}^{*0} e^+ e^-$ with $V = \rho(770)$, $\omega(782)$, $\phi(1020)$, are included explicitly in terms of amplitudes of the decays $\bar{B}^0 \rightarrow \bar{K}^{*0} V$.

Sensitivity of the observables to the choice of form factors of the transition $B \rightarrow K^*$ is also investigated. Various models are chosen in our calculation.

Among all observables we calculate, in particular, the coefficient $A_T^{(2)}$ which determines $\cos(2\phi)$ dependence in the angular distribution of the leptons (ϕ is the angle between the plane spanned by e^+ , e^- and the plane spanned by the decay products K^- , π^+ of the \bar{K}^{*0} meson) and fraction of longitudinal polarization of \bar{K}^{*0} meson.

2 Angular distributions and amplitudes for the $\bar{B}_d^0 \rightarrow \bar{K}^{*0} e^+ e^-$ decay

The decay $\bar{B}_d^0 \rightarrow \bar{K}^{*0} e^+ e^-$ with $\bar{K}^{*0} \rightarrow K^- \pi^+$ on the mass shell is completely described by four independent kinematic variables, the electron-positron pair invariant mass squared, q^2 , and the three angles θ_1 , θ_2 , ϕ . In the helicity frame (Fig. 1), the angle θ_1 (θ_2) is defined as the angle between the directions of motion of e^+ (K^-) in the γ^* (\bar{K}^{*0}) rest frame and the γ^* (\bar{K}^{*0}) in the \bar{B}_d^0 rest frame. The azimuthal angle ϕ is defined as the angle between the decay planes of $\gamma^* \rightarrow e^+ e^-$ and $\bar{K}^{*0} \rightarrow K^- \pi^+$ in the \bar{B}_d^0 rest frame.

The differential decay rate in these coordinates is specified and discussed in Ref. [19]. Having rich multi-dimensional structure, this decay rate is sensitive to various effects modifying the SM, such as CP violation beyond the CKM and/or right-handed currents. Given sufficient data, all bilinear combinations of amplitudes can in principle be completely measured from the full angular distribution in all three angles θ_1 , θ_2 and ϕ .

Here we concentrate on the two-dimensional differential decay rate in q^2 and azimuthal angle ϕ . After integration of fully differential decay rate over the polar angles $\cos \theta_1$ and $\cos \theta_2$, we obtain:

$$\frac{d^2 \Gamma}{d \hat{q}^2 d \phi} = \frac{1}{2\pi} \frac{d \Gamma}{d \hat{q}^2} \left(1 + \frac{1}{2} (1 - f_0) A_T^{(2)} \cos 2\phi - A_{\text{Im}} \sin 2\phi \right), \quad (1)$$

where the electron-positron pairs invariant mass spectrum is

$$\frac{d \Gamma}{d \hat{q}^2} = m_B (|A_0|^2 + |A_{\parallel}|^2 + |A_{\perp}|^2), \quad (2)$$

and coefficients determining angular dependence in (1) are

$$A_T^{(2)} \equiv \frac{f_{\perp} - f_{\parallel}}{f_{\perp} + f_{\parallel}}, \quad A_{\text{Im}} \equiv \frac{\text{Im}(A_{\parallel} A_{\perp}^*)}{\sum_k |A_k|^2}, \quad (3)$$

where the fractions of K^* meson polarization are defined as

$$f_i = \frac{|A_i|^2}{\sum_k |A_k|^2}, \quad f_0 + f_{\parallel} + f_{\perp} = 1 \quad (4)$$

with $i, k = (0, \parallel, \perp)$. Further, m_B is the mass of the B_d^0 meson, $\hat{q}^2 \equiv q^2/m_B^2$, and $A_i A_j^* \equiv A_{iL}(q^2) A_{jL}^*(q^2) + A_{iR}(q^2) A_{jR}^*(q^2)$, where $A_{0L(R)}$, $A_{\parallel L(R)}$ and $A_{\perp L(R)}$ are the complex decay amplitudes of the three helicity states in the transversity basis (see details in [19]).

At present the decay rate (1) is experimentally studied at LHCb [18].

3 Formalism of the $\bar{B}_d^0 \rightarrow \bar{K}^{*0} e^+ e^-$ decay

Within the SM, neglecting contributions proportional to the small CKM factor $V_{us}^* V_{ub}$, the effective Hamiltonian for the quark-level transition $b \rightarrow s e^+ e^-$ is

$$\mathcal{H}_{\text{eff}} = -\frac{4G_F}{\sqrt{2}} V_{ts}^* V_{tb} \left\{ \sum_{i=1}^6 C_i \mathcal{O}_i + C_{7\gamma} \mathcal{O}_{7\gamma} + C_{8g} \mathcal{O}_{8g} + C_{9V} \mathcal{O}_{9V} + C_{10A} \mathcal{O}_{10A} \right\}, \quad (5)$$

where V_{ij} are the CKM matrix elements [20] and G_F is the Fermi coupling constant. We use the operator basis introduced in [21] for the operators \mathcal{O}_i , $i = 1, \dots, 6$, while the remaining ones are given by

$$\mathcal{O}_{7\gamma} = \frac{e}{16\pi^2} \bar{s} \sigma^{\mu\nu} (\bar{m}_b(\mu) P_R + \bar{m}_s(\mu) P_L) b F_{\mu\nu}, \quad (6)$$

$$\mathcal{O}_{8g} = \frac{g_s}{16\pi^2} \bar{s} \sigma^{\mu\nu} (\bar{m}_b(\mu) P_R + \bar{m}_s(\mu) P_L) T^a b G_{\mu\nu}^a, \quad (7)$$

$$\mathcal{O}_{9V} = \frac{\alpha_{\text{em}}}{4\pi} (\bar{s} \gamma_\mu P_L b) \bar{e} \gamma^\mu e, \quad \mathcal{O}_{10A} = \frac{\alpha_{\text{em}}}{4\pi} (\bar{s} \gamma_\mu P_L b) \bar{e} \gamma^\mu \gamma_5 e, \quad (8)$$

where $\alpha_{\text{em}} = e^2/(4\pi) = 1/137$ is the electromagnetic fine-structure constant, g_s is the QCD coupling constant and $P_{L,R} = (1 \mp \gamma_5)/2$ denote chiral projectors. $\bar{m}_b(\mu)$ ($\bar{m}_s(\mu)$) is the running bottom (strange) quark mass in the $\overline{\text{MS}}$ scheme at the scale μ . T^a ($a = 1, \dots, 8$) are the generators of $SU(3)$ color group. Here $F_{\mu\nu}$ and $G_{\mu\nu}^a$ denote the electromagnetic and chromomagnetic field strength tensor, respectively. The Wilson coefficients C_i in Eq. (5) are calculated at the scale $\mu = m_W$, in a perturbative expansion in powers of $\alpha_s(m_W)$ ($\alpha_s(\mu) \equiv g_s^2/(4\pi)$ is the effective QCD coupling constant), and are then evolved down to scales $\mu \sim m_b$ using the renormalization group equations. The $\overline{\text{MS}}$ mass $\bar{m}_b(\mu)$ can be related with the pole mass m_b at the scale $\mu = m_b$ through [22, 23]:

$$\bar{m}_b(m_b) = m_b \left(1 - \frac{4}{3} \frac{\alpha_s(m_b)}{\pi} - 10.167 \left(\frac{\alpha_s(m_b)}{\pi} \right)^2 + \mathcal{O} \left(\left(\frac{\alpha_s(m_b)}{\pi} \right)^3 \right) \right). \quad (9)$$

The up to date value of the strange quark mass is $\bar{m}_s(2 \text{ GeV}) = 95 \pm 25 \text{ MeV}$. Note that this running mass is evaluated at $\mu_0 = 2 \text{ GeV}$ with three active quark flavours. The evolution of the $\bar{m}_s(\mu)$ is governed by the renormalization group equation. It has the solution [24]

$$\frac{\bar{m}_s(\mu)}{\bar{m}_s(\mu_0)} = \frac{f(\alpha_s(\mu)/\pi)}{f(\alpha_s(\mu_0)/\pi)}, \quad \text{with} \quad f(x) = x^{\frac{4}{9}} (1 + 0.895062 x + 1.37143 x^2) + \mathcal{O}(x^4).$$

The matrix element of the effective Hamiltonian Eq. (5) for the non-resonance (NR) decay $\bar{B}_d^0(p) \rightarrow \bar{K}^{*0}(k, \epsilon) e^+(q_+) e^-(q_-)$ can be written, in the so-called naïve factorization [25], as

$$\begin{aligned} \mathcal{M}_{\text{NR}} = & \frac{G_F \alpha_{\text{em}}}{\sqrt{2}\pi} V_{ts}^* V_{tb} \left(\langle \bar{K}^{*0}(k, \epsilon) | \bar{s} \gamma_\mu P_L b | \bar{B}_d^0(p) \rangle (C_{9V}^{\text{eff}} \bar{u}(q_-) \gamma^\mu v(q_+) + C_{10A} \bar{u}(q_-) \gamma^\mu \gamma_5 v(q_+)) \right. \\ & \left. - \frac{2}{q^2} C_{7\gamma}^{\text{eff}} \langle \bar{K}^{*0}(k, \epsilon) | \bar{s} i \sigma_{\mu\nu} q^\nu (\bar{m}_b(\mu) P_R + \bar{m}_s(\mu) P_L) b | \bar{B}_d^0(p) \rangle \bar{u}(q_-) \gamma^\mu v(q_+) \right). \end{aligned} \quad (10)$$

Here, $\sigma_{\mu\nu} = \frac{i}{2} [\gamma_\mu, \gamma_\nu]$, $q_\mu = (q_+ + q_-)_\mu$, $C_{7\gamma}^{\text{eff}} = C_{7\gamma} - (4\bar{C}_3 - \bar{C}_5)/9 - (4\bar{C}_4 - \bar{C}_6)/3$, $C_{9V}^{\text{eff}} = C_{9V} + Y(q^2)$, and the function $Y(q^2)$ is given by [26]

$$\begin{aligned} Y(q^2) = & h(q^2, m_c) (3\bar{C}_1 + \bar{C}_2 + 3\bar{C}_3 + \bar{C}_4 + 3\bar{C}_5 + \bar{C}_6) - \frac{1}{2} h(q^2, m_b) (4\bar{C}_3 + 4\bar{C}_4 + 3\bar{C}_5 + \bar{C}_6) \\ & - \frac{1}{2} h(q^2, 0) (\bar{C}_3 + 3\bar{C}_4) + \frac{2}{9} \left(\frac{2}{3} \bar{C}_3 + 2\bar{C}_4 + \frac{16}{3} \bar{C}_5 \right), \end{aligned} \quad (11)$$

where the “barred” coefficients \bar{C}_i (for $i = 1, \dots, 6$) are defined as certain linear combinations of the C_i , such that the \bar{C}_i coincide at leading logarithmic order with the Wilson coefficients in the standard basis [13]. m_c denotes the pole mass of charm quark. The function

$$h(q^2, m_q) = -\frac{4}{9} \left(\ln \frac{m_q^2}{\mu^2} - \frac{2}{3} - z \right) - \frac{4}{9} (2+z) \sqrt{|z-1|} \begin{cases} \arctan \frac{1}{\sqrt{z-1}} & z > 1, \\ \ln \frac{1+\sqrt{1-z}}{\sqrt{z}} - \frac{i\pi}{2} & z \leq 1, \end{cases} \quad (12)$$

$$h(q^2, 0) = -\frac{4}{9} \ln \frac{q^2}{\mu^2} + \frac{8}{27} + i \frac{4\pi}{9}, \quad (13)$$

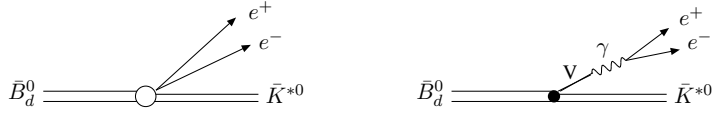


Figure 2. Non-resonant and resonant contributions to the decay amplitude.

with $z = 4m_q^2/q^2$, is related to the basic fermion loop.

The hadronic part of the matrix element in Eq. (10) describing the $B \rightarrow K^* e^+ e^-$ transition can be parameterized in terms of $B \rightarrow K^*$ vector, axial-vector and tensor form factors. The models for the form factors are discussed in [19].

Based on the matrix element in Eq. (10), the non-resonant amplitudes can be written in terms of the vector $V(q^2)$, axial-vector $A_{1,2}(q^2)$ and tensor $T_{1,2,3}(q^2)$ form factors as

$$A_{0L,R}^{\text{NR}} = -\frac{N\hat{\lambda}^{1/4}}{2\hat{m}_{K^*}} \left((C_{9V}^{\text{eff}} \mp C_{10A}) \left((1 - \hat{q}^2 - \hat{m}_{K^*}^2)(1 + \hat{m}_{K^*}) A_1(q^2) - \hat{\lambda} \frac{A_2(q^2)}{1 + \hat{m}_{K^*}} \right) + 2(\hat{m}_b - \hat{m}_s) C_{7\gamma}^{\text{eff}} \left((1 - \hat{q}^2 + 3\hat{m}_{K^*}^2) T_2(q^2) - \frac{\hat{\lambda}}{1 - \hat{m}_{K^*}^2} T_3(q^2) \right) \right), \quad (14)$$

$$A_{\parallel L,R}^{\text{NR}} = N(1 - \hat{m}_{K^*}^2) \sqrt{2\hat{q}^2} \hat{\lambda}^{1/4} \left((C_{9V}^{\text{eff}} \mp C_{10A}) \frac{A_1(q^2)}{1 - \hat{m}_{K^*}} + 2 \frac{\hat{m}_b - \hat{m}_s}{\hat{q}^2} C_{7\gamma}^{\text{eff}} T_2(q^2) \right), \quad (15)$$

$$A_{\perp L,R}^{\text{NR}} = -N \sqrt{2\hat{q}^2} \hat{\lambda}^{3/4} \left((C_{9V}^{\text{eff}} \mp C_{10A}) \frac{V(q^2)}{1 + \hat{m}_{K^*}} + 2 \frac{\hat{m}_b + \hat{m}_s}{\hat{q}^2} C_{7\gamma}^{\text{eff}} T_1(q^2) \right). \quad (16)$$

In the above formulas the definition $\hat{m}_{K^*} \equiv m_{K^*}/m_B$, $\hat{\lambda} \equiv \lambda(1, \hat{q}^2, \hat{m}_{K^*}^2) = (1 - \hat{q}^2)^2 - 2(1 + \hat{q}^2)\hat{m}_{K^*}^2 + \hat{m}_{K^*}^4$, $\hat{m}_b \equiv \bar{m}_b(\mu)/m_B$, $\hat{m}_s \equiv \bar{m}_s(\mu)/m_B$ is used, where m_{K^*} is the mass of the K^{*0} meson, and $N = |V_{tb}V_{ts}^*| G_F m_B^2 \alpha_{\text{em}}/(32\pi^2\sqrt{3}\pi)$.

The transversity amplitudes in (14)–(16) take a particularly simple form in the heavy-quark and large-energy limit. This limit is analyzed in Ref. [19]. It follows from this analysis that in the region of very small invariant masses, $q^2 \ll m_{K^*}^2 = 0.803 \text{ GeV}^2$, the asymmetry $A_{\text{T}}^{(2)}$ in Eq. (3) takes the simple form

$$A_{\text{T}}^{(2)} \approx \frac{2m_s}{m_b}. \quad (17)$$

This result is in agreement with well-known fact, that in the SM for $m_s = 0$ in naïve factorization, $A_{\text{T}}^{(2)} = 0$ [9].

In some extensions of the SM, such as left-right model and unconstrained supersymmetric SM, there are right-handed currents in the matrix element, with the magnitude determined by the coupling $C'_{7\gamma}^{\text{eff}}$ (see, e.g. Ref. [9]). In this case the asymmetry $A_{\text{T}}^{(2)}$ is written as

$$A_{\text{T}}^{(2)} \approx \frac{2C'_{7\gamma}^{\text{eff}} C_{7\gamma}^{\text{eff}}}{(C_{7\gamma}^{\text{eff}})^2 + (C'_{7\gamma}^{\text{eff}})^2}. \quad (18)$$

3.1 Resonant contribution

Next, we implement the effects of LD contributions from the decays $\bar{B}_d^0 \rightarrow \bar{K}^{*0} V$ where $V = \rho^0, \omega, \phi$ mesons, followed by $V \rightarrow e^+ e^-$ in the decay $\bar{B}_d^0 \rightarrow \bar{K}^{*0} e^+ e^-$ (see Fig. 2).

We apply vector-meson dominance (VMD) approach. In general, the $\gamma - V$ transition can be included into consideration using various versions of VMD model. In the “standard” version (see, e.g. [27], chapter 6), the $\gamma - V$ transition vertex can be written as

$$\langle \gamma(\mu) | V(\nu) \rangle = -e f_V Q_V m_V g^{\mu\nu}, \quad (19)$$

where $g^{\mu\nu}$ is the metric tensor, Q_V is the effective electric charge of the quarks in the vector meson: $Q_\rho = \frac{1}{\sqrt{2}}$, $Q_\omega = \frac{1}{3\sqrt{2}}$, $Q_\phi = -\frac{1}{3}$.

The constants f_V can be found from the vector-meson decay width to lepton pair

$$\Gamma(V \rightarrow l^+ l^-) = \frac{4\pi\alpha_{\text{em}}^2}{3} \frac{f_V^2 Q_V^2}{m_V} \left(1 + \frac{2m_l^2}{m_V^2} \right) \sqrt{1 - \frac{4m_l^2}{m_V^2}}. \quad (20)$$

Table 1. Mass, total width, leptonic decay width and coupling f_V of vector mesons [32] (experimental uncertainties are not shown).

V	m_V , MeV	Γ_V , MeV	$\Gamma(V \rightarrow e^+ e^-)$, keV	f_V , MeV
ρ^0	775.49	149.1	7.04	221.3
ω	782.65	8.49	0.60	194.7
ϕ	1019.455	4.26	1.27	228.6

This version of VMD model will be called VMD1. The vertex (19) comes from the transition Lagrangian

$$\mathcal{L}_{\gamma V} = -e A^\mu \sum_V f_V Q_V m_V V_\mu. \quad (21)$$

A more elaborate model (called hereafter VMD2) originates from Lagrangian

$$\mathcal{L}_{\gamma V} = -\frac{e}{2} F^{\mu\nu} \sum_V \frac{f_V Q_V}{m_V} V_{\mu\nu}, \quad (22)$$

where $V_{\mu\nu} \equiv \partial_\mu V_\nu - \partial_\nu V_\mu$ and $F^{\mu\nu} \equiv \partial^\mu A^\nu - \partial^\nu A^\mu$ is the electromagnetic field tensor.

Lagrangian (22) is explicitly gauge invariant, unlike Eq. (21), and gives rise to the $\gamma - V$ vertex

$$\langle \gamma(\mu) | V(\nu) \rangle = -\frac{e f_V Q_V}{m_V} (q^2 g^{\mu\nu} - q^\mu q^\nu), \quad (23)$$

where q is the virtual photon (vector meson) four-momentum. This transition vertex is suppressed at small invariant masses, $q^2 \ll m_V^2$, i.e. in the region far from the vector-meson mass shell¹.

Note that these two versions of the VMD model have been discussed in Refs. [28, 29]. The VMD2 version naturally follows from the Resonance Chiral Theory [30]; in this context VMD2 coupling has been applied in [31] for studying electron-positron annihilation into $\pi^0 \pi^0 \gamma$ and $\pi^0 \eta \gamma$ final states.

Parameters of vector resonances are presented in Table 1.

3.2 Amplitudes for $\bar{B}_d^0 \rightarrow \bar{K}^{*0} V$ decay

An important ingredient of the resonant contribution is amplitude of the decay of B meson into two vector mesons, $B(p) \rightarrow V_1(q, \lambda_1) + V_2(k, \lambda_2)$, with on-mass-shell meson V_2 ($k^2 = m_2^2$) and off-mass-shell meson V_1 ($q^2 \neq m_1^2$).

For the case of two on-mass-shell final mesons one can write the amplitude in the form

$$\mathcal{M} = \Gamma_{\mu\nu} \epsilon_1^{\mu*}(q) \epsilon_2^{\nu*}(k), \quad \Gamma_{\mu\nu} = a g_{\mu\nu} + b p_\mu p_\nu - i c \epsilon_{\mu\nu\alpha\beta} q^\alpha k^\beta \quad (24)$$

in terms of Lorentz scalars a, b, c , $\epsilon_{0123} = +1$, and the four-momenta in the B -meson rest frame are $p^\mu = (m_B, \vec{0})$, $q^\mu = (E_1, 0, 0, |\vec{q}^*|)$, $k^\mu = (E_2, 0, 0, -|\vec{q}^*|)$. We will use the notation $\hat{m}_{1(2)} \equiv m_{1(2)}/m_B$ and put $p^2 = m_B^2$. Conservation of angular momentum requires for the vector-meson helicities $\lambda_1 = \lambda_2 \equiv \lambda$.

Define $H_\lambda \equiv H_{\lambda_1 \lambda_2} = \Gamma_{\mu\nu} \epsilon_1^{\mu*}(\lambda) \epsilon_2^{\nu*}(\lambda)$ and find the relations:

$$H_0 = -\frac{1}{2\hat{m}_1 \hat{m}_2} \left[(1 - \hat{m}_1^2 - \hat{m}_2^2) a + \frac{m_B^2}{2} \lambda(1, \hat{m}_1^2, \hat{m}_2^2) b \right], \quad H_\pm = a \pm \frac{m_B^2}{2} \sqrt{\lambda(1, \hat{m}_1^2, \hat{m}_2^2)} c, \quad (25)$$

with $\lambda(1, \hat{m}_1^2, \hat{m}_2^2) \equiv (1 - \hat{m}_1^2)^2 - 2\hat{m}_2^2(1 + \hat{m}_1^2) + \hat{m}_2^4$.

One can also introduce another set of amplitudes

$$A_{\parallel} = \frac{1}{\sqrt{2}} (H_+ + H_-), \quad A_{\perp} = \frac{1}{\sqrt{2}} (H_+ - H_-), \quad A_0 = H_0, \quad (26)$$

$$A_{\parallel} = \sqrt{2} a, \quad A_{\perp} = m_B^2 \sqrt{\frac{\lambda(1, \hat{m}_1^2, \hat{m}_2^2)}{2}} c, \quad A_0 = -\frac{1}{2\hat{m}_1 \hat{m}_2} \left[(1 - \hat{m}_1^2 - \hat{m}_2^2) a + \frac{m_B^2}{2} \lambda(1, \hat{m}_1^2, \hat{m}_2^2) b \right]. \quad (27)$$

The decay width is expressed as follows:

$$\Gamma(B \rightarrow V_1 V_2) = \frac{m_B}{2} \sqrt{\lambda(1, \hat{m}_1^2, \hat{m}_2^2)} \frac{1}{8\pi m_B^2} (|H_0|^2 + |H_+|^2 + |H_-|^2) = \frac{\sqrt{\lambda(1, \hat{m}_1^2, \hat{m}_2^2)}}{16\pi m_B} \sum_\lambda |A_\lambda|^2. \quad (28)$$

¹The term $\propto q^\mu q^\nu/q^2$ in (23) does not contribute when contracted with the leptonic current

Table 2. Branching ratio [33], and decay amplitudes for $B_d^0 \rightarrow K^{*0} \rho^0$ [34], $B_d^0 \rightarrow K^{*0} \omega$ [34] and $B_d^0 \rightarrow K^{*0} \phi$ [33].

Mode	$K^{*0} \rho^0$	$K^{*0} \omega$	$K^{*0} \phi$
$\text{Br}(B_d^0 \rightarrow K^{*0} V)$	3.4×10^{-6}	2.0×10^{-6}	9.8×10^{-6}
$ h_0^V ^2$	0.70	0.75	0.480
$ h_\perp^V ^2$	0.14	0.12	0.24
$\arg(h_\parallel^V/h_0^V)$ (rad)	1.17	1.79	2.40
$\arg(h_\perp^V/h_0^V)$ (rad)	1.17	1.82	2.39

Table 3. The numerical input used in our analysis. Quark and meson masses are given in GeV.

$ V_{tb}V_{ts}^* $	$G_F, \text{ GeV}^{-2}$	$\mu = m_b$	m_c	$\bar{m}_b(\mu)$	$\bar{m}_s(\mu)$	m_B	m_{K^*}	$\tau_B, \text{ ps}$
0.0407	1.16637×10^{-5}	4.8	1.4	4.14	0.079	5.2795	0.896	1.525

Next, we define the normalized amplitudes:

$$h_\lambda \equiv \frac{A_\lambda}{\sqrt{\sum_{\lambda'} |A_{\lambda'}|^2}}, \quad \sum_\lambda |h_\lambda|^2 = 1 \quad (\lambda, \lambda' = 0, \parallel, \perp). \quad (29)$$

By putting $m_1 = m_V$, $m_2 = m_{K^*}$ and using (28), (29) we obtain the relation between the amplitudes h_λ and A_λ of the process under study $\bar{B}_d^0 \rightarrow \bar{K}^{*0} V$ for any vector meson $V = \rho(770)$, $\omega(782)$, $\phi(1020)$:

$$h_\lambda^V = \frac{1}{4} \lambda^{1/4} (1, \hat{m}_V^2, \hat{m}_{K^*}^2) \sqrt{\frac{\tau_B}{\pi m_B \text{Br}(\bar{B}_d^0 \rightarrow \bar{K}^{*0} V)}} A_\lambda^V, \quad (30)$$

where $\text{Br}(\dots)$ is the branching ratio of $\bar{B}_d^0 \rightarrow \bar{K}^{*0} V$ decay and τ_B is the lifetime of a B meson.

Solving Eqs. (27) we find the scalars a, b and c , and then extend the helicity amplitudes A_λ^V off the mass shell of the meson V , i.e. for $q^2 \neq m_V^2$. We introduce the phases $\delta_\lambda^V \equiv \arg(h_\lambda^V) = \arg(A_\lambda^V)$, and will count the phases of the off-shell amplitudes relative to the phase of h_0^V . Then we have

$$\begin{aligned} A_\parallel^V(q^2) &= |A_\parallel^V| e^{i(\delta_\parallel^V - \delta_0^V)}, & A_\perp^V(q^2) &= \sqrt{\frac{\lambda(1, \hat{q}^2, \hat{m}_{K^*}^2)}{\lambda(1, \hat{m}_V^2, \hat{m}_{K^*}^2)}} |A_\perp^V| e^{i(\delta_\perp^V - \delta_0^V)}, \\ A_0^V(q^2) &= -\frac{1}{4\sqrt{\hat{q}^2} \hat{m}_{K^*}} \left[\sqrt{2}(1 - \hat{q}^2 - \hat{m}_{K^*}^2) |A_\parallel^V| e^{i(\delta_\parallel^V - \delta_0^V)} + \lambda(1, \hat{q}^2, \hat{m}_{K^*}^2) |\hat{b}^V| e^{i(\Phi_b - \delta_0^V)} \right], \\ |\hat{b}^V| &\equiv m_B^2 |b^V| = \frac{\sqrt{2}}{\lambda(1, \hat{m}_V^2, \hat{m}_{K^*}^2)} \left[8\hat{m}_{K^*}^2 \hat{m}_V^2 |A_0^V|^2 + (1 - \hat{m}_V^2 - \hat{m}_{K^*}^2)^2 |A_\parallel^V|^2 \right. \\ &\quad \left. + 4\sqrt{2}\hat{m}_{K^*}\hat{m}_V(1 - \hat{m}_V^2 - \hat{m}_{K^*}^2) |A_0^V| |A_\parallel^V| \cos((\delta_\parallel^V - \delta_0^V)) \right]^{1/2}, \\ \sin(\Phi_b - \delta_0^V) &= -\frac{1}{|\hat{b}^V|} \frac{\sqrt{2}}{\lambda(1, \hat{m}_V^2, \hat{m}_{K^*}^2)} (1 - \hat{m}_V^2 - \hat{m}_{K^*}^2) |A_\parallel^V| \sin((\delta_\parallel^V - \delta_0^V)), \\ \cos(\Phi_b - \delta_0^V) &= -\frac{1}{|\hat{b}^V|} \frac{\sqrt{2}}{\lambda(1, \hat{m}_V^2, \hat{m}_{K^*}^2)} \left[2\sqrt{2}\hat{m}_V\hat{m}_{K^*} |A_0^V| + (1 - \hat{m}_V^2 - \hat{m}_{K^*}^2) |A_\parallel^V| \cos((\delta_\parallel^V - \delta_0^V)) \right]. \end{aligned} \quad (31)$$

Finally, we obtain the total amplitude including non-resonant and resonant parts

$$A_{\lambda L, R} = A_{\lambda L, R}^{NR} + \frac{\alpha_{em} \lambda^{1/4} (1, \hat{q}^2, \hat{m}_{K^*}^2)}{\sqrt{24\pi}} \sum_V \frac{Q_V f_V}{D_V(q^2)} C_{\gamma V} e^{i\delta_\lambda^V} A_\lambda^V(q^2), \quad (32)$$

where $\lambda = (0, \parallel, \perp)$, $C_{\gamma V} = \frac{m_V}{\sqrt{q^2}} \left(\frac{\sqrt{q^2}}{m_V} \right)$ for the VMD1 (VMD2) version, and $D_V(q^2) = q^2 - m_V^2 + im_V \Gamma_V(q^2)$ is the Breit-Wigner function for the V meson resonance shape with the energy-dependent width $\Gamma_V(q^2)$. For details regarding energy-dependent widths see [19].

At present only the amplitudes h_λ^V for $B_d^0 \rightarrow K^{*0} \phi$ decay are known from experiment [33], therefore we use the amplitudes of $B_d^0 \rightarrow K^{*0} \rho$ and $B_d^0 \rightarrow K^{*0} \omega$ decays from theoretical prediction [34]. The absolute values and phases of h_λ^V are shown in Table 2. Other parameters of the model are indicated in Table 3, and the SM Wilson coefficients at the scale $\mu = 4.8$ GeV to NNLO accuracy [11] are shown in Table 4.

Table 4. The SM Wilson coefficients at the scale $\mu = 4.8$ GeV, to NNLO accuracy. Input: $\alpha_s(m_W) = 0.120$, $\alpha_s(\mu) = 0.214$, obtained from $\alpha_s(m_Z) = 0.1176$ using three-loop evolution, $\bar{m}_t(\bar{m}_t) = 162.3$ GeV, $m_W = 80.4$ GeV and $\sin^2 \theta_W = 0.23$.

$C_1(\mu)$	$C_2(\mu)$	$C_3(\mu)$	$C_4(\mu)$	$C_5(\mu)$	$C_6(\mu)$	$C_{7\gamma}^{\text{eff}}(\mu)$	$C_{8g}^{\text{eff}}(\mu)$	$C_{9V}(\mu)$	$C_{10A}(\mu)$
-0.128	1.052	0.011	-0.032	0.009	-0.037	-0.304	-0.167	4.211	-4.103

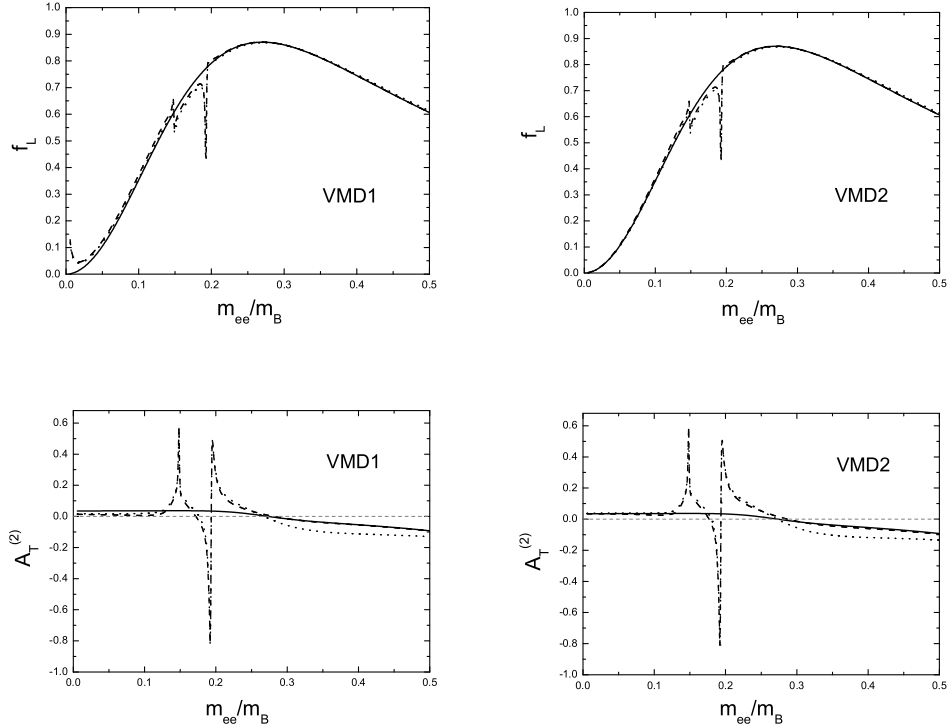


Figure 3. Longitudinal polarization fraction of K^* meson $f_L \equiv f_0$ (upper panels) and transverse asymmetry $A_T^{(2)}$ (lower panels) as functions of m_{ee}/m_B . Left (right) panel corresponds to calculation within VMD1 (VMD2) version of the VMD model. Solid line corresponds to calculation without resonances in the transition form factor model [14]. Dashed and dotted lines are calculations including resonances in the form factor model from [14] and [19] (Eqs. (A7)-(A9) and (A17) there), respectively. The horizontal dashed line indicates zero.

4 Results of calculation for the $\bar{B}_d^0 \rightarrow \bar{K}^{*0} e^+ e^-$ decay and discussion

On Fig. 3 we present results for the invariant mass dependence of a few observables for the $\bar{B}_d^0 \rightarrow \bar{K}^{*0} e^+ e^-$ decay. The upper limit of the invariant mass region, 2.5 GeV, is taken to exclude the contribution from $J/\psi(1S)$ and higher resonances. Of course the presented results may depend on the phase δ_0^V in Eq. (32); for definiteness, we choose $\delta_0^V = 0$ for all resonances ρ , ω and ϕ .

In general, the resonances ρ , ω and ϕ show up as irregularities on the smooth non-resonant background. There is practically no dependence of longitudinal polarization fraction f_L on the choice of form factors. At very small m_{ee} this observable shows a sensitivity to the version of the VMD model.

The asymmetry coefficient $A_T^{(2)}$ in Eq. (7) is more sensitive to the form factor model. Addition of the resonances change considerably this observable. The resonant contribution depends on the version of the VMD model, in particular, at invariant mass below 0.5 GeV (where $q^2 \ll m_{K^*}^2$), in the VMD2 version, $A_T^{(2)}$ is about 0.04 which is in agreement with Eq. (17). While in the VMD1 version, the resonances influence $A_T^{(2)}$ even at small m_{ee} .

Note, that the dependence of $A_T^{(2)}$ on the mass of the strange quark has been studied in [19], and it appeared to be important. Indeed, comparison of $A_T^{(2)}$ for $m_s = 0$ and $m_s \neq 0$ demonstrates effect of the “wrong” helicity transition $b_L \rightarrow s_R + \gamma_R$. In the SM this effect is proportional to $2m_s/m_b$ (see Eq. (17)), while in some extensions of the SM it can reach bigger values depending on the coefficient $C_{7\gamma}^{\text{eff}}$ in Eq. (18).

5 Conclusions

The rare FCNC decay $\bar{B}_d^0 \rightarrow \bar{K}^{*0} (\rightarrow K^- \pi^+) e^+ e^-$ has been studied in the region of electron-positron invariant mass below $\bar{c}c$ threshold. Main emphasis has been put on an accurate account of the mechanism $\bar{B}_d^0 \rightarrow \bar{K}^{*0} (\rightarrow K^- \pi^+) V$ with low lying vector resonances $V = \rho(770), \omega(782), \phi(1020)$ decaying into the $e^+ e^-$ pair.

The invariant mass dependence of the coefficient $A_T^{(2)}$ in the azimuthal angle distribution of the lepton pair has been calculated and studied.

In view of the current experiments on LHCb, in which the integrated over invariant mass observables will be measured [18], we have also calculated the corresponding quantities [19]. Two integration regions have been selected which are particularly suitable for the planned future measurements on LHCb [18]. The predictions for integrated observables are given in framework of the SM with account of low lying vector resonances.

Acknowledgements. A.Yu. K. is grateful to the Organizers of NPQCD-2011 School-Seminar for invitation and kind hospitality in Dnepropetrovsk.

References

- [1] M. Antonelli, D.M. Asner, D. Bauer, et al., Phys. Rept. **494** 197 (2010) [arXiv:0907.5386v1 [hep-ph]].
- [2] R. Ammar *et al.*, [CLEO Collaboration], Phys. Rev. Lett. **71**, 674 (1993).
- [3] A. Ali and A.Ya. Parkhomenko, Eur. Phys. J. C **23**, 89 (2002).
- [4] S.W. Bosch and G. Buchalla, Nucl. Phys. B **621**, 459 (2002).
- [5] D. Atwood, M. Gronau, and A. Soni, Phys. Rev. Lett. **79**, 185 (1997); B. Grinstein, Y. Grossman, Z. Ligeti, and D. Pirjol, Phys. Rev. D **71**, 011504 (2005); D. Atwood, T. Gershon, M. Hazumi, and A. Soni, Phys. Rev. D **71**, 076003 (2005).
- [6] Y. Grossman and D. Pirjol, JHEP **06**, 029 (2000).
- [7] D. Melikhov, N. Nikitin, and S. Simula, Phys. Lett. B **442**, 381 (1998); F. Krüger, L.M. Seghal, N. Sinha, and R. Sinha, Phys. Rev. D **61**, 114028 (2000); Phys. Rev. D **63**, 019901(E) (2001); C.S. Kim, Y.G. Kim, C.-D. Lu, and T. Morozumi, Phys. Rev. D **62**, 034013 (2000).
- [8] A. Ali, P. Ball, L.T. Handoko, and G. Hiller, Phys. Rev. D **61**, 074024 (2000); A. Ali, E. Lunghi, C. Greub, and G. Hiller, *ibid.* D **66**, 034002 (2002).
- [9] F. Krüger and J. Matias, Phys. Rev. D **71**, 094009 (2005).
- [10] C. Bobeth, G. Hiller, and G. Piranishvili, JHEP **07**, 106 (2008); U. Egede, T. Hurth, J. Matias, M. Ramon, and W. Reece, *ibid.* **11**, 032 (2008).
- [11] W. Altmannshofer, P. Ball, A. Bharucha, A.J. Buras, D.M. Straub, and M. Wick, JHEP **01**, 019 (2009).
- [12] U. Egede, T. Hurth, J. Matias, M. Ramon, and W. Reece, arXiv:1005.0571v1.
- [13] G. Buchalla, A.J. Buras, and M.E. Lautenbacher, Rev. Mod. Phys. **68**, 1125 (1996).
- [14] P. Ball and R. Zwicky, Phys. Rev. D **71**, 014029 (2005).
- [15] F. De Fazio, T. Feldmann, and T. Hurth, Nucl. Phys. B **733**, 1 (2006); Erratum-*ibid.* B **800**, 405 (2008); JHEP **0802**, 031 (2008).
- [16] B. Aubert *et al.*, (The BABAR Collaboration), Phys. Rev. Lett. **102**, 091803 (2009).
- [17] J.-T. Wei *et al.*, (The Belle Collaboration), Phys. Rev. Lett. **103**, 171801 (2009).
- [18] J. Lefrancois and M.H. Schune, LHCb-PUB-2009-008, 2009.
- [19] A.Yu. Korchin and V.A. Kovalchuk, Phys. Rev. D **82**, 034013 (2010) [arXiv:1004.3647 [hep-ph]].
- [20] N. Cabibbo, Phys. Rev. Lett. **10**, 531 (1963); M. Kobayashi and T. Maskawa, Prog. Theor. Phys. **49**, 652 (1973).
- [21] K. Chetyrkin, M. Misiak, and M. Münz, Phys. Lett. B **400**, 206 (1997); E: B **425**, 414 (1998).
- [22] N. Gray, D.J. Broadhurst, W. Grafe, and K. Schilcher, Z. Phys. C **48**, 673 (1990).
- [23] K.G. Chetyrkin and M. Steinhauser, Phys. Rev. Lett. **83**, 4001 (1999); K. Melnikov and T. van Ritbergen, Phys. Lett. B **482**, 99 (2000).
- [24] K.G. Chetyrkin, Phys. Lett. B **404**, 161 (1997); J.A.M. Vermaasen, S.A. Larin, and T. van Ritbergen, Phys. Lett. B **405**, 327 (1997).
- [25] T. Hurth, Int. J. Mod. Phys. A **22**, 1781 (2007).
- [26] M. Beneke, Th. Feldmann, and D. Seidel, Nucl. Phys. B **612**, 25 (2001).
- [27] R.P. Feynman, *Photon-hadron interactions*, W.A. Benjamin, Inc. Reading, Massachusetts, 1972.
- [28] F. Klingl, N. Kaiser, and W. Weise, Z. Phys. A **356**, 193 (1996) [arXiv:hep-ph/9607431].
- [29] H.B. O'Connell, B.C. Pearce, A.W. Thomas, and A.G. Williams, Prog. Nucl. Part. Phys. **39** (1997) 201.
- [30] G. Ecker, J. Gasser, A. Pich, and E. de Rafael, Nucl. Phys. B **321** (1989) 311.
- [31] S. Eidelman, S. Ivashyn, A. Korchin, G. Pancheri, and O. Shekhovtsova, Eur. Phys. J. C **69**, 103 (2010).
- [32] K. Nakamura *et al.* (Particle Data Group), J. Phys. G **37**, 075021 (2010).
- [33] Heavy Flavor Averaging Group (HFAG), <http://www.slac.stanford.edu/xorg/hfag/rare/>.
- [34] C.H. Chen, arXiv:hep-ph/0601019v2.